HHS Public Access

Author manuscript

NMR Biomed. Author manuscript; available in PMC 2024 June 01.

Published in final edited form as:

NMR Biomed. 2023 June ; 36(6): e4698. doi:10.1002/nbm.4698.

Prospects and limitations of paramagnetic chemical exchange saturation transfer agents serving as biological reporters in vivo

A. Dean Sherry[1,2], **Daniela Delli Castelli**[3], **Silvio Aime**[3]

[1]Department of Chemistry and Biochemistry, University of Texas at Dallas, Richardson, Texas, USA

[2]Advanced Imaging Research Center, University of Texas Southwestern Medical Center, Dallas, Texas, USA

[3]Department of Molecular Biotechnology and Health Sciences, University of Turin, Turin, Italy

Abstract

The concept of using paramagnetic metal ion complexes as chemical exchange saturation transfer agents (paraCEST) for molecular imaging of various biological processes first appeared in the literature about 20 years ago. The first paraCEST agent was based on a highly shifted, inner-sphere, slowly exchanging water molecule that could be activated at a frequency far away from bulk water, a substantial advantage for selective activation of the agent alone. Many other paraCEST agent designs followed that were based on activation of exchanging -NH or -OH proton on the chelate itself. Both types of paraCEST designs are attractive for molecular imaging because the rates of water molecule or ligand proton exchange can be designed to be sensitive to a biological or physiological property such as pH, enzyme activity, or redox. Hence, the intensity or frequency of the resulting CEST signal provides a direct readout of that property. Many molecular designs have appeared in the literature over the past 20 years, mostly reported as proof-of-concept designs but, unfortunately, only a few reports have explored the limitations of paraCEST agents for imaging a biological process in vivo. As a community, we now know that the sensitivity of paraCEST agents is lower than one might anticipate based upon simple chemical exchange principles and, in general, it appears the sensitivity of paraCEST agents is even lower in vivo than in vitro. In this short review, we address some of the factors that contribute to the limited sensitivity of paraCEST agents in vivo, offer some thoughts on approaches that could lead to dramatically improved paraCEST sensitivity, and challenge the scientific community to perform more in vivo experiments designed to test these ideas.

Keywords

chemical exchange; molecular imaging; paraCEST; responsive MR agents

Correspondence A. Dean Sherry, Department of Chemistry and Biochemistry, University of Texas at Dallas, Richardson, TX 75080, USA. dean.sherry@utsouthwestern.edu.

1 | INTRODUCTION

The emergence of paramagnetic lanthanide complexes as paramagnetic chemical exchange saturation transfer (paraCEST) agents naturally evolved with the discovery of CEST and a nearly 50-year history on the use of lanthanides as NMR shift reagents (SRs).[1] Given the basic CEST requirement ($\Delta\omega \geq k_{ex}^2$), it was obvious that one should be able to take advantage of the SR properties of lanthanide complexes to extend $\Delta\omega$ and thereby expand the chemical types of exchanging protons (faster k_{ex}) that meet the CEST requirement. A second advantage to expanding $\Delta\omega$ was that this moves the CEST activation frequency farther away from water protons, thereby eliminating or at least reducing any off-resonance saturation effects of CEST activation. There are two different types or classes of paraCEST agents, those based on an exchanging water molecule and a much broader category of paraCEST agents based upon exchanging protons on a chelating ligand, typically -NH, -OH protons (Figure 1). This article is not intended to be a comprehensive review of all types of paraCEST agents reported in the literature but rather provide an overview of the current status of both classes of paraCEST agents plus nanoparticle-derived agents and provide a critical discussion of current issues/controversies associated with their use in vivo. Although most of the examples provided here focus on studies involving lanthanide-bases paraCEST systems, it should be pointed out that transition metal-based systems have also been widely reported.[3] Nevertheless, the prospects and limitations we outline here also apply to those systems.

2 | WATER-BASED PARACEST AGENTS

The first reported water-based paraCEST agent[4] was EuDOTA-$(gly)_4^-$, a complex that displays a separate ^1H signal near 50 ppm for the single inner-sphere water molecule on the Eu^{3+} ion. This surprising observation indicated that water exchange was unexpectedly slow in this complex, slow enough to allow transfer of saturated proton spins from the water molecule on the Eu^{3+} ion to bulk water (i.e., CEST). This observation opened the door to an avalanche of reports describing a variety of water-based paraCEST agents for sensing glucose,[5,6] pH,[7] redox,[8] Zn^{2+} ions,[9] and other biological indices of interest. Each of these reports described new EuDOTA-derivatives with differing water exchange rates that become altered in response to some biological parameter of interest. For example, the EuDOTA-bis-phenylboronate complex[5] used for sensing glucose showed an increase in CEST intensity when complexed with glucose because the bound glucose interfered with the exchanging water molecule and decreased the rate of water exchange. The redox-sensitive EuDOTA-bis (quinolinium) complexes[8] were also based on differences in water exchange rates, with the oxidized (NAD^+) form showing faster water exchange than the reduced (NADH) form. These two examples illustrate the simplicity and ease of creating new responsive CEST agents based on changes in water exchange rates. Many other water-based paraCEST agents have been reported since then but very few have moved beyond simple in vitro demonstrations. So, one might ask, why have so few water-based paraCEST agents been applied in vivo? Does this simply reflect the fact that chemists who design such agents do not have ready access to small animal MR scanners or are there other chemical features of these agents that limit in vivo applications?

Several factors may contribute to the limited success of water-based paraCEST agents in vivo. First, water molecule exchange must be quite slow in these complexes, not only to meet the CEST requirement ($\Delta\omega \geq k_{ex}$), but also to achieve optimal CEST. The intensity of a CEST signal (M_z/M_o) depends upon many factors, including agent concentration, temperature, the T_1 of bulk water protons, exchange rate (k_{ex}) and applied power, B_1. Figure 2 illustrates the relationship between water residence lifetime, τ_M ($1/k_{ex}$ and applied B_1, so if one is B_1 limited by scanner limitations or concerns about sample heating, then an agent with slower water exchange would be needed to achieve optimal CEST. All of the water-based paraCEST agents referenced above respond to the biological parameter of interest by a change in k_{ex} (slowing or speeding up water exchange), but, in the design of such agents, less consideration was given to whether k_{ex} was optimal for CEST detection. Bloch theory predicts that optimal CEST can be achieved if the rate of water exchange matches the applied power, $k_{ex} = 2\pi B_1$,[10] so for a prototype paraCEST agent such as EuDOTA-$(gly)_4^-$ with a water exchange rate of ~5000 s^{-1} at 25°C, a B_1 of 795 Hz (18.7 μT) would be required for optimal CEST. This example illustrates one of the major limitations of water-based paraCEST agents: water exchange must be even slower than most of the agents reported so far to be useful at an acceptable B_1 power level. The slowest water exchange rate reported so far for any EuDOTA-based paraCEST agent was 1360 s^{-1} (measured in vitro at 298 K),[11] so the power requirement for optimal CEST using that agent is 5.1 μT, a more acceptable power for in vivo application. Most of the other published examples of water-based paraCEST agents display water exchange rates that are adequate for in vitro demonstration but are generally too fast for in vivo applications.

A second factor is that the water exchange rate in these complexes may differ in vivo compared with that measured in vitro. The vast majority of paraCEST complexes reported in the literature were studied at temperatures near 25°C, even although the physiological temperature in vivo is ~37°C. The impact of this 12° difference can be quite dramatic for water-based paraCEST systems. For example, the water exchange rate in EuDOTA-$(gly)_4^-$ varies 10-fold between 10°C (1136 s^{-1}) and 37°C (10,752 s^{-1}),[12] so the CEST signal of this agent is much weaker at 37°C (water exchange is too fast). Water exchange can also be impacted by the biological milieu. For example, the CEST intensity of EuDOTA-(t-butylamide)$_4^{4+}$ was reportedly 40% lower when dissolved in plasma compared with aqueous buffer at the same temperature. This likely reflects binding interactions between this hydrophobic agent and plasma proteins that catalyze faster water molecules when bound to a protein.[14] The CEST properties of series of Co (II), Fe (II), and Ni (II) complexes derived from N_2O_3 macrocycles with two appended acetamide groups have also been shown to differ in aqueous buffer, agarose, egg white, and rabbit serum, with proton exchange rates varying up to 13-fold in these different media.[13] Given that CEST originates from the exchanging amide protons in these complexes, the sensitivity of CEST to environment must be ascribed to the presence of nucleophilic anions or proteins that initiate prototropic exchange. The impact of prototropic exchange on CEST can be easily demonstrated in vitro by adding anionic buffers to catalyze proton exchange,[15] but the extent to which this reduces the CEST sensitivity of these agents in vivo is largely unknown.

3 | PROTON-BASED PARACEST AGENTS

Shortly after the first report of EuDOTA-$(gly)_4^-$ as a water-based CEST agent, Aime et al. demonstrated that the four tetra-glycinate amide protons on the ligand itself could also be used for CEST activation.[16] The advantages of using -NH protons for CEST activation are 2-fold: (1) amide protons exchange more slowly than inner-sphere water molecules (hence lower B_1 power is needed for optimal saturation); and (2) -NH proton exchange is base-catalyzed so the CEST signal from -NH protons is nearly always pH-dependent. A comparison of the CEST properties of a series of LnDOTA-$(gly)_4^-$ complexes showed that the Yb^{3+} complex produced the largest CEST signal from the -NH protons, so by preparing a mixture of EuDOTA-$(gly)_4^-$ and YbDOTA-$(gly)_4^-$, they demonstrated that one could activate CEST from the bound water molecule in EuDOTA-$(gly)_4^-$ (independent of pH between 5.5 and 8.0), then, in a second measurement, activate CEST from the four equivalent -NH protons of YbDOTA-$(gly)_4^-$ at an entirely different frequency (highly pH-dependent) and use the ratio of the two CEST signals as a direct readout of pH (Figure 3).[16] In a later report, Terreno et al.[17] demonstrated that pH can be measured using PrDOTA-$(gly)_4^-$ by ratiometric CEST activation of the water versus the -NH protons in this single complex. In one early in vivo study, a novel ytterbium-based agent, Yb-DO3A-oAA, with two chemically distinct types of -NH protons (amide and amine), used the ratio of CEST signals from those two proton exchange sites to estimate the distribution of extracellular pH in a MCF-7 mammary carcinoma grown in the flank of mouse.[18] Given that this measurement could only be accomplished after direct injection of the agent into the tumor, the general utility of this agent for imaging tissue pH in vivo seems to be limited. However, two other TmDO3A-peptide derivatives have been used to measure specific enzyme activities in vitro[19] and in vivo[20] using ratiometric CEST methods so the general utility of paraCEST agents with two different chemical types of exchanging protons cannot be discounted. These early reports stimulated reports of other paraCEST agent designs as pH reporters, including many different types of transition metal ion complexes.[13,21,22] Although transition metal ion-based paraCEST agents may ultimately prove safer for use in humans compared with lanthanide-based agents, none have been tested or even studied in animals in vivo at this point.

The most successful in vivo application of a small molecule paraCEST agent to date is arguably YbHPDO3A, a stable macrocyclic complex used for imaging tissue pH.[23] This Yb-complex consists of the same macrocyclic ligand, hydroxypropyl-DO3A, used in the clinically approved Gd-based agent, ProHance®. CEST activation of this complex occurs through the exchanging -OH proton directly coordinated to the Yb^{3+} ion. Given that YbHPDO3A is present in solution as a mixture of two coordination isomers each displaying unique chemical shifts, a separate CEST signal is generated by activation of the two well-resolved -OH proton resonances (Figure 4). Surprisingly, the -OH proton exchange rates in the two coordination isomers differ slightly and, as a result, each CEST signal shows a different pH sensitivity. Consequently, the ratio of the two CEST signals is also sensitive to pH and identical in both aqueous buffer and in serum.[24] Thus, the CEST ratio, independent of agent concentration, was used to successfully image tissue pH in a U87 glioma mouse model[24] and in a melanoma murine model[25] after bolus injection of 1.2 mmol/kg agent.

That dose, ~10-fold higher than the typical clinical dose of ProHance, highlights one of the current limitations of small molecule paraCEST agents. Although the two -OH exchange peaks were clearly distinguishable by CEST MRI at this concentration, the background MT signal in both tumor models dominates the signal in both tumor models. Hence, separating out the true ratiometric CEST values from the underlying broad MT signal presents a second limitation. Nonetheless, both in vivo studies using YbHP-DO3A as a pH sensor reported that the extracellular pH in both tumor models was heterogeneous, as anticipated.

In another in vivo study, a water-based paraCEST agent, in which the frequency of the exchanging water molecule changes in response to a change in pH, was used.[26] This alternative design should in principle offer an advantage over ratiometric CEST designs because pH is reported directly in a single CEST spectrum by measuring the frequency of the exchanging water molecule. Figure 5 shows the structure of the agent, a calibration curve of CEST frequency versus pH in aqueous buffer (red) and plasma (blue), and a single voxel CEST spectrum collected from the kidney of a mouse 6 min after tail vein injection of 0.4 mmol/kg agent. One advantage of using the kidney as a target tissue for imaging pH is that low molecular weight agents such as this are quickly cleared by renal filtration so are naturally concentrated in this organ. The clearly detected CEST exchange peak near ~47 ppm should in principle provide a direct readout of pH in that voxel but the width of the exchange peak was quite variable in vivo, ranging from 6.3 to 14.5 ppm, so the uncertainty in the measured pH value in each voxel is large and variable. This shows that for frequency-dependent paraCEST agents to be useful in vivo, proton or water molecule exchange that gives rise to CEST must be much slower. This illustrates the advantages of using more slowly exchanging -OH or -NH proton species for frequency-dependent CEST measurements. Some promising new candidates that could potentially fulfill this requirement include YbHP-DO3P^{3-} (with CEST arising from a single directly coordinated -OH group near +130 ppm)[27] and the transition metal ion-based agent, FeTAPC^{2+} (with CEST arising from four equivalent -NH_2 groups near −74 ppm).[22] Further studies will be needed to determine whether these agents retain their promising features in vivo.

Both ratiometric CEST and frequency-dependent CEST should, in principle, report tissue pH values independent of agent concentration. Nonetheless, given that an independent gold standard measure of tissue pH is not available (other than inserting a micro-pH electrode), it is difficult to judge the accuracy of the pH values reported by CEST. The pH gradient across normal functioning kidneys has been well established for many years[28] so one could consider a well-functioning kidney as a gold standard reference for testing the efficacy of new agents. Given that existing paraCEST agents have been only partially successful in reporting the known pH gradient across functioning kidneys, there is a need for further detailed studies to determine why such agents do not seem to report correct pH values in vivo. Do the many other exchanging protons in vivo alter the CEST signal in unexpected ways? Does the ever-present MT signal modify in vitro calibration curves of CEST response versus pH? Or, can these differences be ascribed to incomplete B_1 or B_0 corrections to pH maps collected in vivo?

The dominating MT signal that contributes heavily to the CEST signal in most tissues has been an incentive for many laboratories to design paraCEST agents with exchanging proton

or water signals well outside the typical MT window (~ ± 100 ppm). For example, Wang et al.[29] prepared a dibutyl-phosphonate ester derivative of the ligand shown in Figure 5 to slow water exchange even further and replaced the Eu^{3+} ion with a Tb^{3+} ion to move the water-based CEST signal well downfield of the tissue MT signal. Even although the complex has some attractive features, limitations in the water solubility of the resulting Tb^{3+} agent precluded further in vivo testing of this molecule. Similarly, several cobalt (II) proton-based paraCEST complexes have been shown to have CEST exchange peaks well outside the typical broad MT profile.[21] It should be pointed out that the chemical shift of these paramagnetically shifted peaks are extremely sensitive to temperature so setting up an animal scanner to locate the correct activation frequency can at times be quite difficult.

4 | SOME RECENT CHEMICAL INSIGHTS MAY PROVE USEFUL IN AMPLIFYING THE CEST SIGNAL OF SMALL MOLECULE PARACEST AGENTS

A recent report described how to combine the advantages of using a directly coordinated -OH proton for CEST activation (ala YbHP-DO3A) in an agent that also displays a pH-dependent chemical shift.[27] This was accomplished by substituting the three carboxyl groups in HP-DO3A with phosphonate groups to yield HP-DO3P. This chemical modification altered the molecular features of the agent in multiple ways. First, the phosphonate substitutions resulted in exclusion of the inner-sphere exchanging water molecule in YbHP-DO3P^{3-}, thereby reducing the impact of T_{2ex} on the water linewidth. Second, the bulkier phosphonate groups resulted in a single TSAP coordination isomer for YbHP-DO3P^{3-} compared with two isomers for YbHP-DO3A. The more nucleophilic phosphonate oxygen atoms also resulted in larger Yb-induced chemical shifts of all protons in the complex including the exchanging -OH proton resonance, which was shifted downfield well beyond the broad underlying MT signal and, unexpectedly, the -OH CEST peak in YbHP-DO3P^{3-} was also significantly sharper, indicating that proton exchange is slower in this complex. This is clearly a significant advantage because less power is required for CEST activation. Finally, the three phosphonate groups in YbHP-DO3P^{3-} undergo protonated/deprotonated between pH 4 and 9 and this alters the chemical shift of all protons in the molecule, including the exchanging -OH proton. The net result of this simple chemical modification was that the sharp -OH CEST peak provided a direct readout of pH with little to no interference from the broad MT signal. One unanticipated feature of this agent after infusion into mice was its unusually long blood half-life. Even although the reasons for this extended blood half-life are yet to be unraveled, this feature may prove advantageous for delivery of the agent into the extracellular space of tumors for direct pH measurements.

Where do we go from here as a CEST community? It seems clear that paraCEST agents are less sensitive in vivo than in vitro but the reasons for this difference appears to be quite variable. What impact does the presence of hundreds of exchanging proton species in tissues have on the sensitivity of paraCEST agents? Can we find ways to amplify the sensitivity of paraCEST agents through prototropic exchange mechanisms? A recent report by Baroni et al.[30] may provide some useful insights. In that study, Baroni et al. demonstrated that the presence of a basic site (carboxyl or amine, see Figure 6) in proximity to the hydroxyl group

of Ln (HP-DO3A) allows for formation of a H-bond with the coordinated -OH group that provides a pathway for intramolecular proton exchange and an enhanced CEST signal. For example, very little CEST was observed in EuHP-DO3A because -OH proton exchange is too slow, while CEST was increased by ~10-fold in Eu-Bz-HP-DO3A and by nearly 40-fold in Eu-An-HP-DO3A.[30] This demonstrates that formation of an intramolecular H-bonding network with an exchanging -OH proton used for CEST activation can substantially increase the sensitivity of a paraCEST agent. This exciting observation could lead to new designs that bring the sensitivity of small molecule paraCEST agents like those described above into competition with existing Gd-based T_1 agents.

5 | AMPLIFICATION BY MULTIPLEXING

An alternative approach to improving the sensitivity of small molecule paraCEST agents is to maximize the local concentration of these agents using various types of nanocarriers such as micelles, polymers, and other nanoparticles. Many examples of these strategies have been reported in the literature but only a few examples will be discussed here.

5.1 | Micelles

Micelles consist of self-assembled amphiphilic molecules containing a hydrophobic moiety linked to a hydrophilic group. The hydrophobic part is typically constituted by a linear aliphatic or polymeric chain and the hydrophilic motif contains at least one or more polar groups that ensure a good affinity with water molecules. Upon forming the supramolecular aggregation, the molecules are arranged in such a way as to minimize the contact between the hydrophobic chains and the water. In fact, the amphiphilic molecules are organized according to a radial structure with the hydrophobic chains inside and the hydrophilic groups outside in contact with the solvent. Usually, micelles range in size from 10 to 100 nm. These systems are considered strategic nanomedicine platforms for both therapeutic and diagnostic applications thanks to their in vivo stability, ability to solubilize water-insoluble drugs, and prolonged blood circulation times. Zhu et al.[31] developed a thermo-sensitive nanosized paraCEST MRI contrast agent using a copolymer of poly N-isopropylacrylamide block methyl methacrylate with two different length chains known to undergo a sharp morphological change in structure over a narrow range near physiological temperatures. In this case, the water-based paraCEST agent, EuDOTA-4AmCE, was attached to the short chain polymer component, and when the temperature was below 37°C, the longer chains embedded the Eu^{3+} complex in the interior of the micelle, thereby partially “quenching” their CEST response. However, above 37°C, the shorter chains become more exposed to bulk water and consequently the CEST signal increased in intensity by ~20%. This method appears to have great potential for the detection of temperature changes in different tissues as the responsiveness of the system covers a range of temperatures of physiopathological interest. The CEST signal intensity remains concentration-dependent but delivery of such a temperature-dependent micelle to a target of interest would allow monitoring of temperature changes in that tissue location.

A second example involved the synthesis of a long-chain HP-DO3A ligand that spontaneously forms micelles in solution.[32] In this design, the polar head group consisted

of a mixture of Eu (III)/Yb (III)-HPDO3A derivatives attached to alkyl chains of 16 carbon atoms. A comparison of CEST signal intensities between monomers and micelles showed that the micelles were ~200 times more sensitive, yet, importantly, the pH-responsive properties associated with these paraCEST probes remained nearly unchanged. This again is important because targeting such paraCEST-based micelles to a specific target, such as a tumor in vivo, should allow monitoring of extracellular pH in those regions. A similar increase in CEST sensitivity was achieved for water-based paraCEST complexes that spontaneously form micelles.[33] By comparison of amphiphilic EuDOTA-tetraamide systems having variable alkyl chain lengths (C1, C12, C14, and C16), it was found that an increase in chain length not only resulted in an increase in micelle size, as expected, but unexpectedly also decreased the water exchange rate. This resulted in an increase in effectiveness of these paraCEST-based micelles for detection at physiological temperatures.

5.2 | Dendrimers

The word dendrimer comes from the Greek word “dendron”, which means “tree”. Dendrimers are molecules consisting of a central nucleus from which branches extend radially, with each branch ending with the same functional group. The number of branches defines the dendrimer's generation (G) that progressively increases branching after branching (G1, G2, G3 …). These systems display a high degree of molecular uniformity, tunable size, and multivalency potential. Owing to these properties, dendrimers have been intensively studied as drug delivery systems and for multiplexing paraCEST agents. Gruell et al.[34] developed Yb (III)DOTAM-functionalized poly (propylene imine) dendrimers of different generations and, as expected, the CEST sensitivity increased in proportion to the number of YbDOTAM units per dendrimer. The authors observed that upon increasing the dendrimer generation, the pH-dependence of the CEST effect slightly shifted towards a more acidic pH range. A possible explanation for the observed behavior was proposed to rely on the presence of a strong basic microenvironment associated with the multiple tertiary amine groups of the dendritic core. This feature paves the way for the design of fine-tuned systems for the determination of pH in different pathological states by modulating the dendrimer scaffold.

A few years later, Ali et al.[35] demonstrated the feasibility of using paraCEST agents conjugated to dendrimers for in vivo CEST MRI evaluation of the pharmacokinetics of nanoparticles. In this case, the chosen dendrimers were a generation 2 and a generation 5 polyamidoamine (G2PAMAM/G5PAMAM) conjugated with Yb $(DOTA\text{-}gly)_4^-$ or Eu $(DOTA\text{-}gly)_4$,- respectively (ref. Eu/YbGly). The detection limit for these systems was found to be 0.045 and 0.242 mM for Eu-G5 and Yb-G2, respectively. The dendrimeric agents were injected into a mouse model of mammary carcinoma. An increase in the CEST effect in the tumor region was measured by irradiating the specific water exchange frequency of each agent. The ratio between the CEST signals of Eu-G5 versus Yb-G2, measured over a period of time, was used to assess the relative in vivo pharmacokinetics of the two nanoparticles of different size. As anticipated, the CEST response revealed that the larger dendrimer (Eu-G5) accumulated less in tumors compared with the smaller Yb-G2, but, due to slower elimination of the larger species, the larger dendrimer maintained an enhanced CEST signal in the tumor over time (Figure 7). Three years later, the same

group reported the use of a dual probe (optical and paraCEST MRI) to validate the in vivo detection of these dendrimeric paraCEST agents.[36] They synthetized a fluorescent/paraCEST MRI contrast agent by conjugating EuDOTA-$(gly)_4$ and a fluorescent dye (DyLight® 680) to a G5PAMAM dendrimer. This probe was tested in a U87 glioma model. A strong CEST effect was visualized immediately postinjection at the tumor rim, and the effect persisted during the remainder of the MRI study for the next 50 min. A comparison of either in vivo or ex vivo fluorescence imaging data validated the CEST data, confirming accumulation of the probe in the glioma.

5.3 | Silica Nanoparticles

During the last 2 decades, inorganic nanoparticles have attracted great attention in the biomedical field thanks to their chemical stability and mechanical strength. Many studies have demonstrated that inorganic nanoparticles such as mesoporous silica nanoparticles are among the most convenient drug delivery systems because of their high surface area, large pore volume, biocompatibility, tunable pore size, and easily functional surface.[37] One of the early attempts to create a highly sensitive paraCEST silica nanoparticle was reported by Evbuomwan et al.,[38] who attached ~1200 EuDOTA-$(gly)_4^-$ molecules to the surface of amine-modified 50-nm nanoparticles via one of the extended glycine carboxylate groups. Disappointingly, the resulting CEST spectra of these modified silica nanoparticles showed complete elimination of the Eu^{3+}-bound water CEST peak normally found near 50 ppm accompanied by excess broadening of the bulk water signal. These features could be explained by catalysis of the protons from the slowly exchanging Eu^{3+}-bound water molecule by the excess positively charged amino groups on the surface of the nanoparticles effectively quenching the bound-water CEST signal.

Quite a different result was observed by Ferrauto et al.[39] after anchoring a similar number of LnDO3A complexes (where Ln = Eu, Tm, Tb) to the surface of MCM-41 mesoporous silica nanoparticles (20–50 nM in size), again modified by surface amino groups (Figure 8). As in the previous study, the LnDO3A complexes were linked to the surface amine groups via a single carboxylate group of DO3A. Although the LnDO3A complexes are not paraCEST agents themselves because the rate of water molecule exchange is too rapid, the hypothesis tested was whether surface silanol (Si–OH) groups would bind to the inner sphere of the Ln ion in the attached LnDO3A complexes and convert them into LnHP-DO3A-like proton-based paraCEST agents. Given that the number of Si–OH groups present on the surface of the functionalized silica was estimated to be two per nm^2, the probability of these surface -OH groups interacting with the attached LnDO3A complexes was quite high. Indeed, the CEST spectra of the products showed a broadened -OH proton exchange CEST peak with maxima near 5.5, 7.5, and 15 ppm for Eu–, Tm–, and Tb– nanoparticles, respectively. Although the chemical shifts of these exchanging -OH protons were substantially smaller than the corresponding LnHP-DO3A complexes (indicative of averaging multiple exchanging -OH protons), the CEST sensitivity of these nanoparticles was dramatically higher (in the μM range per Ln ion) compared with the corresponding molecular systems. This remarkable result suggests that multiple Si–OH groups may be interacting with each surface-bound LnDO3A complex thereby providing a unique mechanism to amplify the CEST signal several thousand-fold. The process has yet to

be optimized but has the potential to convert small silica nanoparticles into highly sensitive multicolored paraCEST sensors, somewhat analogous to quantum dots.

Some years later, Carniato et al.[40] compared the CEST properties of two mesoporous silica nanoparticles (MCM-41 and SBA-15) differing only in the location of anchored TbDO3A complexes. In the case of MCM-41, the Tb chelates were distributed on the external surface or at the entrance to the pores whereas, in the case of SBA-15, the complexes were located mainly inside the channels. Both systems yielded CEST signals ascribed to the silanol -OH groups in proximity to the anchored TbDO3A complexes, hence turning them into paraCEST complexes, as reported previously.[39] They found, however, that the sensitivity of the MCM-41 particle was one order of magnitude larger (55 ± 5 μM) than the SBA-15 particle and ascribed the difference to limited diffusion of water molecules into the pore channels to reach the paramagnetic centers. This study nicely demonstrates the importance of probe location in creating the most sensitive nanoparticles of this type.

5.4 | Perfluorocarbon Nanoparticles

These systems consist of a liquid perfluorocarbon core surrounded by a monolayer of surfactants ranging in size from 200 to 300 nm. They are biologically inert and highly stable. Owing to their very large surface area, it is possible to load them with large amounts of imaging agents, targeting ligands, or drugs. Like other nanosystems, perfluorocarbon nanoparticles represent a versatile platform for different biomedical applications. Winter et al.[41] incorporated very high payloads of a lipid-conjugated Eu^{3+} methoxy-benzyl-DOTA) chelate onto the surface of a perfluorcarbon-based nanoparticle and demonstrated that the CEST spectrum of this nanosized particle displayed a bound water peak near 52 ppm with exchange properties similar to those of the small molecule paraCEST agents dissolved in an aqueous solution. These nanoparticles were further functionalized with an antifibrin antibody and targeting experiments on blood clots were performed. A contrast-to-noise ratio of 10% was detected thus supporting the view that the system could be a potential imaging agent for the detection of fibrin deposits in unstable atherosclerotic plaques.

5.5 | Virus-like particles

Over the past 2 decades, many virus-like particles have been considered in the design of efficient drug and gene delivery systems. Virus-inspired nanocarriers have the advantage, over other nanosystems, of mimicking viral infection machineries, that is, allowing for their peculiar immune system evasion, tissue tropism, cell entry, and endosomal escape. Vasalatiy et al.[42] labeled recombinant adenovirus type 5 particles (AdCMVLuc) with a derivative of TmDOTAM and found that the Tm-adenovirus conjugate with 1140 thulium ions per adenovirus particle retained their ability to infect cells and deliver a luciferase gene. A 12% decrease in bulk water signal intensity was observed for the paraCEST-coated virus particles relative to controls. This result demonstrated the possibility of using virus-like particles as carriers for functionally active paraCEST agents for imaging delivery of virus particles to cells.

5.6 | SupraCEST systems

An additional route to nanosystems that has been exploited for improving the sensitivity of paraCEST agents relies on the formation of noncovalent supramolecular adducts (supraCEST) between a paramagnetic SR and a substrate acting as source of mobile protons.[43] The idea was to use a diamagnetic polyaminoacid endowed with a large number of residual positive charges and exchanging protons to set up multiple electrostatic interactions with a negatively charged paramagnetic SR. In this study, the cationic polypeptide poly-L-arginine (53.5 kDa) was used and the negatively charged lanthanide complex $TmDOTP^{5-}$ was used to shift the shift guanidine proton resonances well downfield of the bulk water resonance. In the absence of the paramagnetic complex, at pH = 7.4, the solution containing poly-L-arginine at 110 μM did not display a significant CEST signal but, upon addition of $TmDOTP^{5-}$ (18-fold molar excess), a supramolecular adduct was formed, which resulted in an intense CEST peak near ~30 ppm reflecting the downfield-shifted arginine protons. It is likely that the H-bonding associated with formation of the supramolecular adduct results in a decrease in the exchange rate of arginine mobile protons and hence is more favorable for CEST. Establishing H-bonds with the functionality providing the pool of exchanging protons is a general rule to decrease the exchange rate. The sensitivity threshold of this system was in the micromolar range (a CEST effect of 5% was observed when the concentration of polymer was 1.7 μM and that of the SR was 30 μM, at neutral pH). Although the SR and the poly-arginine were not covalently attached and would likely dissociate in vivo, the concept of using novel supraCEST systems such as this to amplify the sensitivity of paraCEST detection into an acceptable level for molecular imaging in vivo is a fundamentally important concept.

5.7 | Cyclodextrins

Cyclodextrins (CDs) are a family of cyclic oligosaccharides with a hydrophilic outer surface and a lipophilic inner cavity. As soon as the structure and properties of cyclodextrins became known (around the middle of the 20th century), interest in these systems focused mainly on exploring their ability to form inclusion complexes with various hydrophobic molecules that can be hosted into their toroidal or cone-shaped inner cavity. In drug delivery applications, CDs have mainly been used as complexing agents to increase the solubility of hydrophobic drugs and to increase their bioavailability and stability. As CDs contain a relatively high number of exchanging protons, they were considered good candidates as a substrate for the design of supraCEST systems. Pereira et al.[44] reported a paramagnetic supraCEST formed between positively charged CDs, CDs bearing ammonium groups at the upper rim (CD+), and the negatively charged SR, $TmDOTP^{5-}$. Formation of the supramolecular adduct resulted in greater resolution of the bulk water and amine proton signals, thus making the latter pool of exchanging protons detectable by CEST. The magnitude of this chemical shift difference was considerably smaller than that found in the Tm/Arg supraCEST system because in the Tm−/CD+ system, $TmDOTP^{5-}$ was found to be located 10–11 Å above the center of the CD + cavity. Nonetheless, this study provided the first example of the use of CDs to create a highly sensitive supraCEST system.

A second example of the use of CDs to create a unique CEST platform was recently described by Goren et al.,[45] who designed a set of lanthanide-cradled α-cyclodextrins (Ln-

CDs) able to host (on reversible host–guest binding dynamics) fluorinated molecules. The ^{19}F resonance of the guest undergoes a lanthanide-induced shift while in the cage, thereby making it possible to observe two distinct^{19}F signals for the bound and unbound substrate. By changing the lanthanide ion or the molecular structure of the host, it is possible to obtain a huge library of ^{19}F signals that can be selectively irradiated to yield the corresponding ^{19}F CEST signals. This demonstrates the feasibility of a switchable, polychromatic palette for multicolor-mapping. The proposed system, called paraGEST by analogy, does not appear suitable for in vivo diagnostic applications but the authors suggested a novel application in the field of molecular steganography, called CODE-HD, where the number of color display permutations resulting from one library of nine pseudocolors is 387,420,489 (9^9 when arranged in a 3 × 3 well plate, Figure 9). The potential advantage of this method over the existing technologies based on luminescence relies on the possibility of observing artificial colors whenever the use of light is difficult (i.e., opaque objects or media with strong light scattering).

6 | SUMMARY, CONCLUSIONS, AND RECOMMENDATIONS

The concept of paraCEST arose shortly after the discovery of CEST by the single observation that lanthanide complexes can be created that exhibit extremely slow water molecule exchange kinetics, so slow in fact that a separate resonance for a Ln-bound water molecular can be detected by high-resolution ^1H NMR spectroscopy. This observation, quite remarkable at the time, quickly led to other paraCEST designs, where paramagnetically shifted -NH, -OH protons on various ligands housing the paramagnetic ion can be used as efficient CEST antenna. In general, paraCEST is also attractive for the development of frequency-encoding systems for the simultaneous detection of multiple agents in the same anatomical region. The possibility of modulating either the chemical shift or exchange rate of the pool of exchanging protons is undoubtedly a property that makes these systems ideal CEST agents. Unfortunately, less attention has been given to optimizing the CEST signal from these novel agents than creating new paraCEST systems. Consequently, only a few agents have been demonstrated to work in vivo. The biological medium is a very important determinant of the efficacy of the CEST experiment, as the complex buffering composition of the cell has a significant impact on all proton exchange processes, including those involving paraCEST agents. There comes a time when a scientific field must focus on the practical development of new imaging agents such as those described here and less on other new designs. We as a community should discourage more proof-of-concept publications and turn our attention to solving the limitations of paraCEST agents in general. If we fail to do this, the scientific community will soon lose interest and the funding of paraCEST projects will diminish. The opportunities to turn our existing knowledge of paraCEST agents and amplification systems into practical tools remains unlimited.

ACKNOWLEDGEMENTS

We gratefully acknowledge funding from the National Institutes of Health (R01 CA115531) and the Italian Ministry of University and Research (MUR and PRIN projects) in support of this project.

Abbreviations used:

paraCEST	paramagnetic chemical exchange saturation transfer
SR	shift reagent
supraCEST	supramolecular adduct between a SR and a substrate acting as a source of mobile protons

REFERENCES

1. Geraldes CFGC. Lanthanide Shift Reagents. In: Atwood DA, ed. The Rare Earth Elements: Fundamentals and Applications. Wiley & Sons; 2012:501–520.
2. Ward KM, Aletras AH, Balaban RS. A new class of contrast agents for MRI based on proton chemical exchange dependent saturation transfer (CEST). J Magn Reson. 2000;143(1):79–87. doi:10.1006/jmre.1999.1956 [PubMed: 10698648]
3. Morrow JR, Chowdhury MSI, Abozeid SM, Patel A, Raymond JJ. Transition Metal ParaCEST, LipoCEST, and CellCEST Agents as MRI Probes. In: Encyclopedia of Inorganic and Bioinorganic Chemistry:1–19.
4. Zhang S, Winter P, Wu K, Sherry AD. A novel europium (III)-based MRI contrast agent. J Am Chem Soc. 2001;123(7):1517–1518. doi:10.1021/ja005820q [PubMed: 11456734]
5. Zhang S, Trokowski R, Sherry AD. A paramagnetic CEST agent for imaging glucose by MRI. J Am Chem Soc. 2003;125(50):15288–15289. doi:10.1021/ja038345f [PubMed: 14664562]
6. Ren J, Trokowski R, Zhang S, Malloy CR, Sherry AD. Imaging the tissue distribution of glucose in livers using a PARACEST sensor. Magn Reson Med. 2008;60(5):1047–1055. doi:10.1002/mrm.21722 [PubMed: 18958853]
7. Wu Y, Soesbe T, Kiefer GE, Zhao P, Sherry AD. A responsive europium (III) chelate that provides a direct readout of pH by MRI. J Amer Chem Soc. 2010;132:14002–14003. doi:10.1021/ja106018n [PubMed: 20853833]
8. Ratnakar SJ, Viswanathan S, Kovacs Z, Jindal AK, Green KN, Sherry AD. Europium (III) DOTA-tetraamide complexes as redox-active MRI sensors. J Am Chem Soc. 2012;134(13):5798–5800. doi:10.1021/ja211601k [PubMed: 22420507]
9. Trokowski R, Ren J, Kálmán FK, Sherry AD. Selective sensing of zinc ions with a PARACEST contrast agent. Angew Chem Int Ed. 2005;44(42):6920–6923. doi:10.1002/anie.200502173
10. Woessner DE, Zhang S, Merritt ME, Sherry AD. Numerical solution of the Bloch equations provides insights into the optimum design of PARACEST agents for MRI. Magn Reson Med. 2005;53(4):790–799. doi:10.1002/mrm.20408 [PubMed: 15799055]
11. Fernando WS, Martins AF, Zhao P, et al. Breaking the barrier to slow water exchange rates for optimal magnetic resonance detection of paraCEST agents. Inorg Chem. 2016;55(6):3007–3014. doi:10.1021/acs.inorgchem.5b02850 [PubMed: 26937683]
12. Dixon WT, Ren J, Lubag AJ, et al. A concentration-independent method to measure exchange rates in PARACEST agents. Magn Reson Med. 2010;63(3):625–632. doi:10.1002/mrm.22242 [PubMed: 20187174]
13. Olatunde AO, Cox JM, Daddario MD, Spernyak JA, Benedict JB, Morrow JR. Seven-coordinate coII, feII and six-coordinate niII amide-appended macrocyclic complexes as paraCEST agents in biological media. Inorg Chem. 2014;53(16):8311–8321. doi:10.1021/ic5006083 [PubMed: 24820102]
14. Ali MM, Woods M, Suh EH, et al. Albumin-binding PARACEST agents. JBIC J Biol Inorg Chem. 2007;12(6):855–865. doi:10.1007/s00775-007-0240-z [PubMed: 17534672]
15. Liepinsh E, Otting G. Proton exchange rates from amino acid side chains—implications for image contrast. Magn Reson Med. 1996;35(1):30–42. doi:10.1002/mrm.1910350106 [PubMed: 8771020]
16. Aime S, Barge A, Delli Castelli D, et al. Paramagnetic lanthanide (III) complexes as pH-sensitive chemical exchange saturation transfer (CEST) contrast agents for MRI applications. Magn Reson Med. 2002;47(4):639–648. doi:10.1002/mrm.10106 [PubMed: 11948724]

17. Terreno E, Castelli DD, Cravotto G, Milone L, Aime S. Ln (III)-DOTAMGly complexes: a versatile series to assess the determinants of the efficacy of paramagnetic chemical exchange saturation transfer agents for magnetic resonance imaging applications. Invest Radiol. 2004;39(4):235–243. doi:10.1097/01.rli.0000116607.26372.d0 [PubMed: 15021328]
18. Liu G, Li Y, Sheth VR, Pagel MD. Imaging in vivo extracellular pH with a single paramagnetic chemical exchange saturation transfer magnetic resonance imaging contrast agent. Mol Imaging. 2012;11(1):47–57. doi:10.2310/7290.2011.00026 [PubMed: 22418027]
19. Hingorani DV, Randtke EA, Pagel MD. A catalyCEST MRI contrast agent that detects the enzyme-catalyzed creation of a covalent bond. J Am Chem Soc. 2013;135(17):6396–6398. doi:10.1021/ja400254e [PubMed: 23601132]
20. Yoo B, Sheth VR, Howison CM, et al. Detection of in vivo enzyme activity with CatalyCEST MRI. Magn Reson Med. 2014;71(3):1221–1230. doi:10.1002/mrm.24763 [PubMed: 23640714]
21. Dorazio SJ, Olatunde AO, Spernyak JA, Morrow JR. CoCEST: cobalt (ii) amide-appended paraCEST MRI contrast agents. Chem Commun. 2013;49(85):10025–10027. doi:10.1039/c3cc45000g
22. Tsitovich PB, Cox JM, Spernyak JA, Morrow JR. Gear up for a pH shift: a responsive iron (II) 2-amino-6-picolyl-appended macrocyclic paraCEST agent that protonates at a pendent group. Inorg Chem. 2016;55(22):12001–12010. doi:10.1021/acs.inorgchem.6b02159 [PubMed: 27934305]
23. Delli Castelli D, Terreno E, Aime S. YbIII-HPDO3A: a dual pH- and temperature-responsive CEST agent. Angew Chem Int Ed. 2011;50(8):1798–1800. doi:10.1002/anie.201007105
24. Ferrauto G, Di Gregorio E, Auboiroux V, et al. CEST-MRI for glioma pH quantification in mouse model: Validation by immunohistochemistry. NMR Biomed. 2018;31(11):e4005. doi:10.1002/nbm.4005 [PubMed: 30256478]
25. Delli Castelli D, Ferrauto G, Cutrin JC, Terreno E, Aime S. In vivo maps of extracellular pH in murine melanoma by CEST–MRI. Magn Reson Med. 2014;71(1):326–332. doi:10.1002/mrm.24664 [PubMed: 23529973]
26. Wu Y, Zhang S, Soesbe TC, et al. pH imaging of mouse kidneys in vivo using a frequency-dependent paraCEST agent. Magn Reson Med. 2016;75(6):2432–2441. doi:10.1002/mrm.25844 [PubMed: 26173637]
27. Ratnakar SJ, Chirayil S, Funk AM, et al. A frequency-selective pH-responsive paraCEST agent. Angew Chem Int Ed. 2020;59(48):21671–21676. doi:10.1002/anie.202008888
28. Burke TJ, Malhotra D, Shapiro JI. Factors maintaining a pH gradient within the kidney: role of the vasculature architecture. Kidney Int. 1999;56(5):1826–1837. doi:10.1046/j.1523-1755.1999.00738.x [PubMed: 10571791]
29. Wang X, Wu Y, Soesbe TC, et al. A pH-responsive MRI agent that can be activated beyond the tissue magnetization transfer window. Angew Chem Int Ed. 2015;54(30):8662–8664. doi:10.1002/anie.201502497
30. Baroni S, Carnovale IM, Carrera C, et al. H-bonding and intramolecular catalysis of proton exchange affect the CEST properties of EuIII complexes with HP-DO3A-like ligands. Chem Commun. 2021;57(26):3287–3290. doi:10.1039/D1CC00366F
31. Zhu X, Chen S, Luo Q, Ye C, Liu M, Zhou X. Body temperature sensitive micelles for MRI enhancement. Chem Commun. 2015;51(44):9085–9088. doi:10.1039/C5CC02587G
32. Ferrauto G, Beauprez F, Di Gregorio E, et al. Development and characterization of lanthanide-HPDO3A-C16-based micelles as CEST-MRI contrast agents. Dalton Trans. 2019;48(16):5343–5351. doi:10.1039/C8DT04621B [PubMed: 30942212]
33. Evbuomwan OM, Kiefer G, Sherry AD. Amphiphilic EuDOTA-tetraamide complexes form micelles with enhanced CEST sensitivity. Eur J Inorg Chem. 2012;2012(12):2126–2134. doi:10.1002/ejic.201101369 [PubMed: 23378821]
34. Pikkemaat JA, Wegh RT, Lamerichs R, et al. Dendritic PARACEST contrast agents for magnetic resonance imaging. Contrast Media Mol Imaging. 2007;2(5):229–239. doi:10.1002/cmmi.149 [PubMed: 17937448]
35. Ali MM, Yoo B, Pagel MD. Tracking the relative in vivo pharmacokinetics of nanoparticles with PARACEST MRI. Mol Pharm. 2009;6(5):1409–1416. doi:10.1021/mp900040u [PubMed: 19298054]

36. Ali MM, Bhuiyan MP, Janic B, et al. A nano-sized PARACEST-fluorescence imaging contrast agent facilitates and validates in vivo CEST MRI detection of glioma. Nanomedicine. 2012;7(12):1827–1837. doi:10.2217/nnm.12.92 [PubMed: 22891866]
37. Chen Y, Chen H, Shi J. In vivo bio-safety evaluations and diagnostic/therapeutic applications of chemically designed mesoporous silica nanoparticles. Adv Mater. 2013;25(23):3144–3176. doi:10.1002/adma.201205292 [PubMed: 23681931]
38. Evbuomwan OM, Merritt ME, Kiefer GE, Sherry AD. Nanoparticle-based PARACEST agents: the quenching effect of silica nanoparticles on the CEST signal from surface-conjugated chelates. Contrast Media Mol Imaging. 2012;7(1):19–25. doi:10.1002/cmmi.459 [PubMed: 22344876]
39. Ferrauto G, Carniato F, Tei L, Hu H, Aime S, Botta M. MRI nanoprobes based on chemical exchange saturation transfer: LnIII chelates anchored on the surface of mesoporous silica nanoparticles. Nanoscale. 2014;6(16):9604–9607. doi:10.1039/C4NR02753A [PubMed: 25029466]
40. Carniato F, Ferrauto G, Muñoz-Úbeda M, Tei L. Water diffusion modulates the CEST effect on Tb (III)-mesoporous silica probes. Magnetochemistry. 2020;6(3):38 doi:10.3390/magnetochemistry6030038
41. Winter PM, Cai K, Chen J, et al. Targeted PARACEST nanoparticle contrast agent for the detection of fibrin. Magn Reson Med. 2006;56(6):1384–1388. doi:10.1002/mrm.21093 [PubMed: 17089356]
42. Vasalatiy O, Gerard RD, Zhao P, Sun X, Sherry AD. Labeling of adenovirus particles with PARACEST agents. Bioconjug Chem. 2008;19(3):598–606. doi:10.1021/bc7002605 [PubMed: 18254605]
43. Aime S, Delli Castelli D, Terreno E. Supramolecular adducts between poly-L-arginine and [TmIIIdotp]: a route to sensitivity-enhanced magnetic resonance imaging-chemical exchange saturation transfer agents. Angew Chem Int Ed Engl. 2003;42(37):4527–4529. doi:10.1002/anie.200352132 [PubMed: 14520757]
44. Pereira GA, Peters JA, Terreno E, et al. Supramolecular adducts of negatively charged lanthanide (III) DOTP chelates and cyclodextrins functionalized with ammonium groups: mass spectrometry and nuclear magnetic resonance studies. Eur J Inorg Chem. 2012;2012(12):2087–2098. doi:10.1002/ejic.201101201
45. Goren E, Avram L, Bar-Shir A. Versatile non-luminescent color palette based on guest exchange dynamics in paramagnetic cavitands. Nat Commun. 2021;12(1):3072. doi:10.1038/s41467-021-23179-9 [PubMed: 34031377]

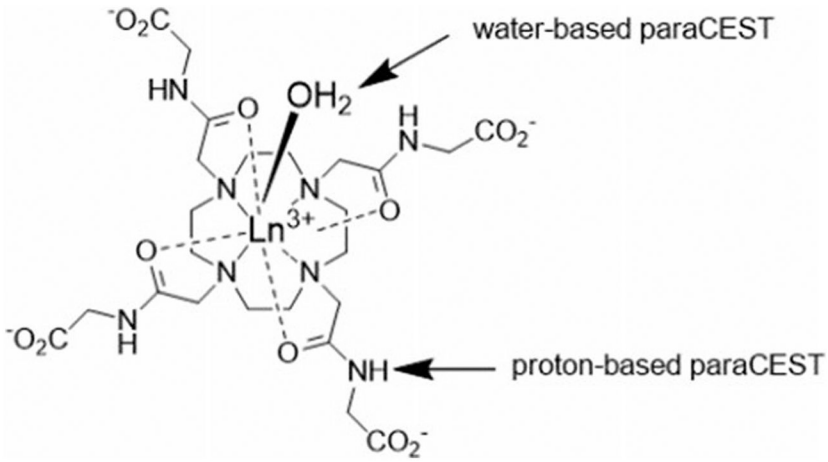

FIGURE 1.

An example chemical structure of a general paramagnetic chemical exchange saturation transfer (paraCEST) agent illustrating the difference between a water-based versus a proton-based CEST agent

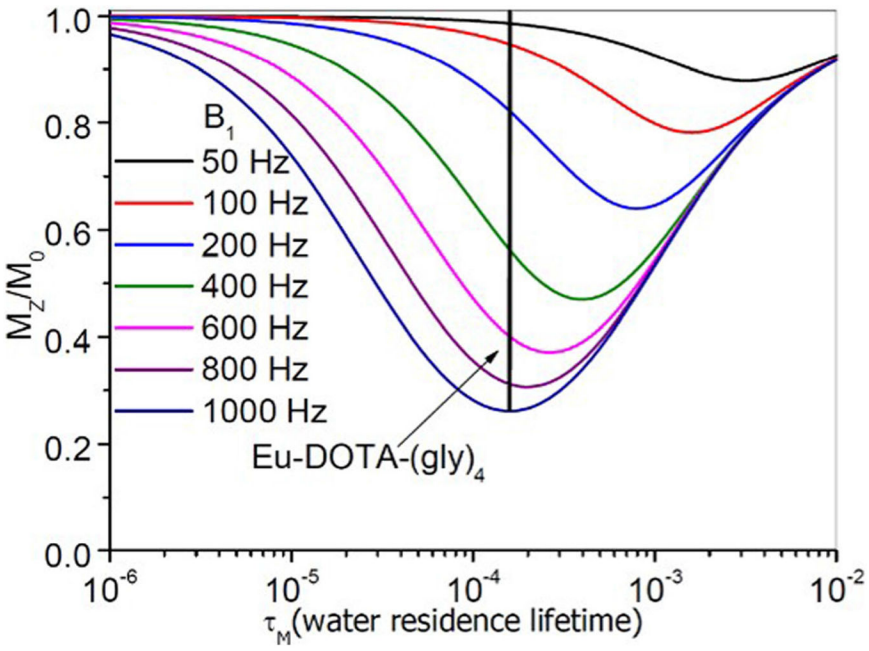

FIGURE 2.

A plot of M_z/M_0 versus water residence lifetime ($1/k_{ex}$) derived from the Bloch equations[10]

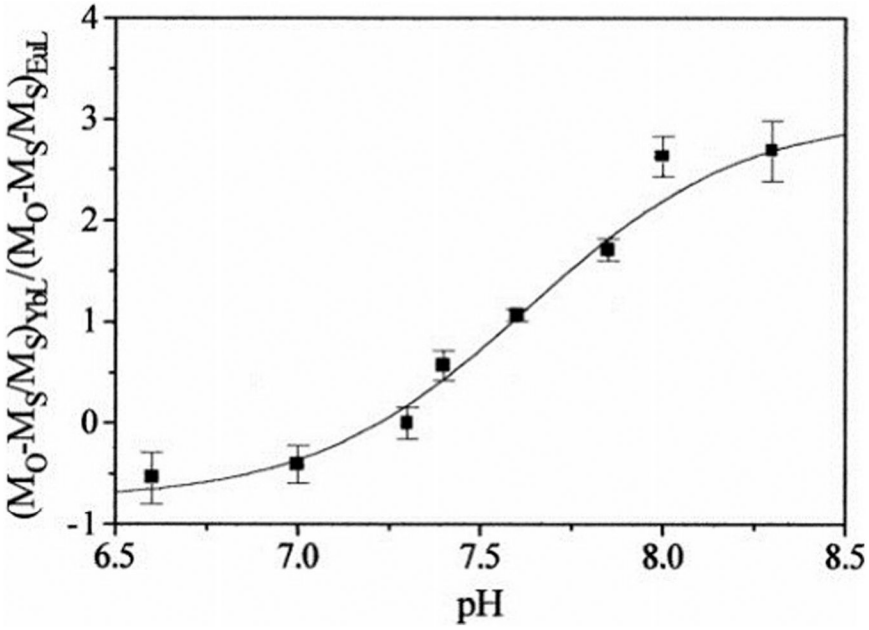

FIGURE 3.

A ratiometric plot of the chemical exchange saturation transfer signals of two different agents (Yb/Eu) versus pH (adapted from[16])

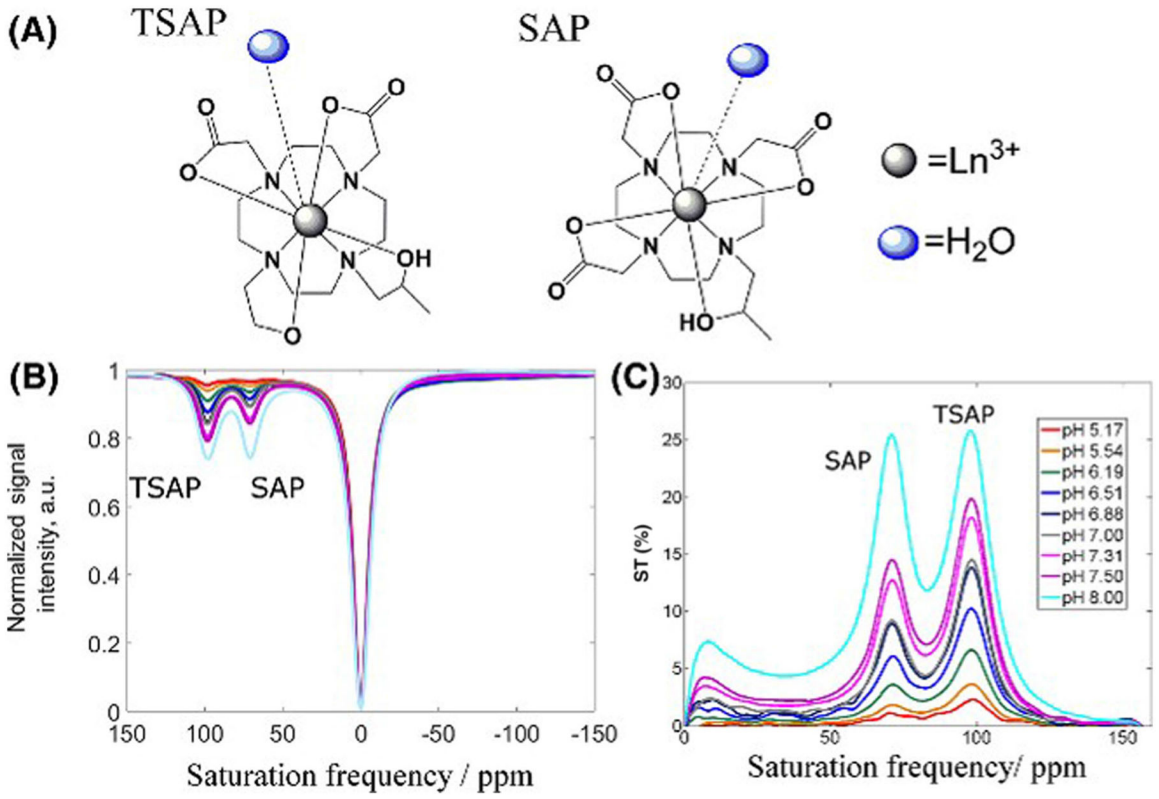

FIGURE 4.

Chemical structures of the TSAP (twisted square antiprism) and SAP (square antiprism) isomers of YbHP-DO3A (A). The CEST spectra (B and C) demonstrate that the two isomers differ in pH sensitivity so the ratio of the two CEST intensities provides a direct readout of pH (reproduced from[23])

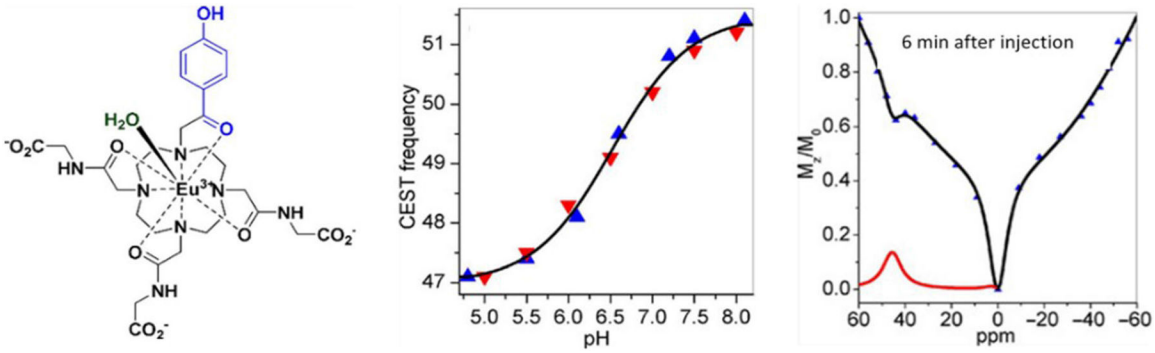

FIGURE 5.

A water-based paramagnetic chemical exchange saturation transfer (paraCEST) agent that reports pH by direct readout of the frequency of the exchanging water molecule. The chemical structure, calibration curve, and detection of the water exchange CEST peak in the mouse kidney 6 min after intravenous injection (reproduced from three different figures from[26])

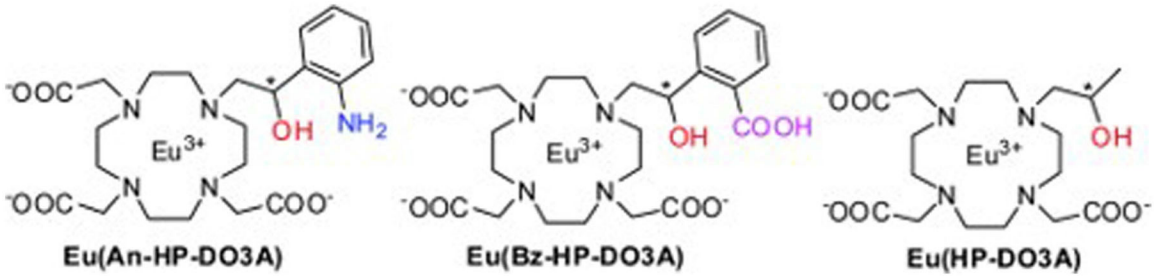

FIGURE 6.

The chemical structures of two derivatives of Eu (HP-DO3A) with intramolecular proton donor or acceptor groups situated near the exchanging -OH proton (in red) (reproduced from[30])

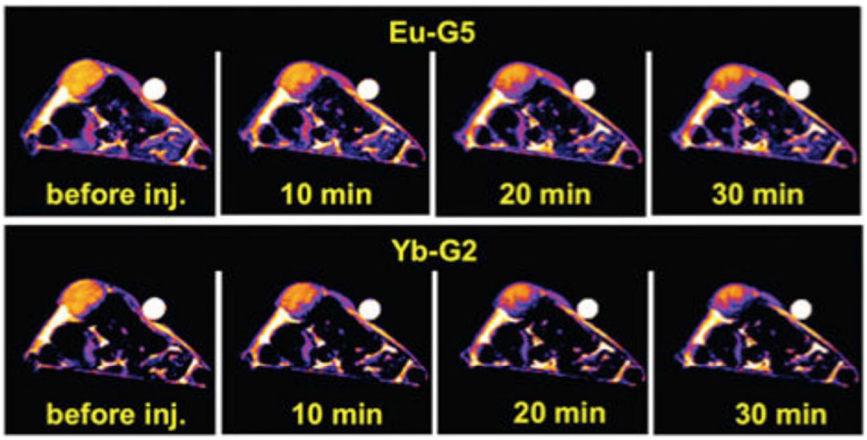

FIGURE 7.

Eu-G5 and Yb-G2 were injected into the blood of a mouse-bearing MCF-7 mammary carcinoma in its flank. Axial MR images were acquired by applying a 20-μT saturation pulse for 2.25 s before a RARE-16 MR signal acquisition period. Selective saturation was applied at the frequency of each paraCEST agent (adapted from[35])

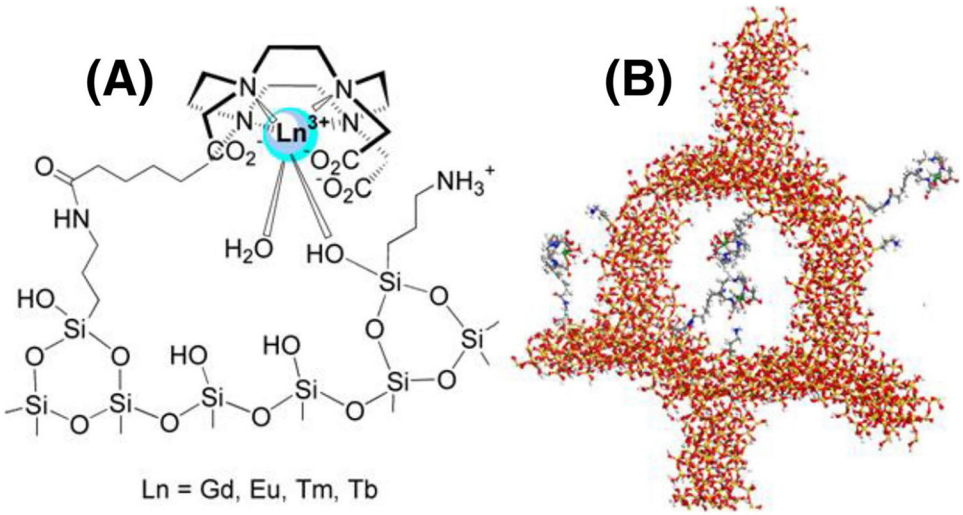

FIGURE 8.

Schematic representation of (A) The interaction between LnDO3A-like chelates and the surface of the organo-modified MCM-41, and (B) Ln (III) chelates anchored on the organo-modified mesoporous silica nanoparticles (reproduced from[39])

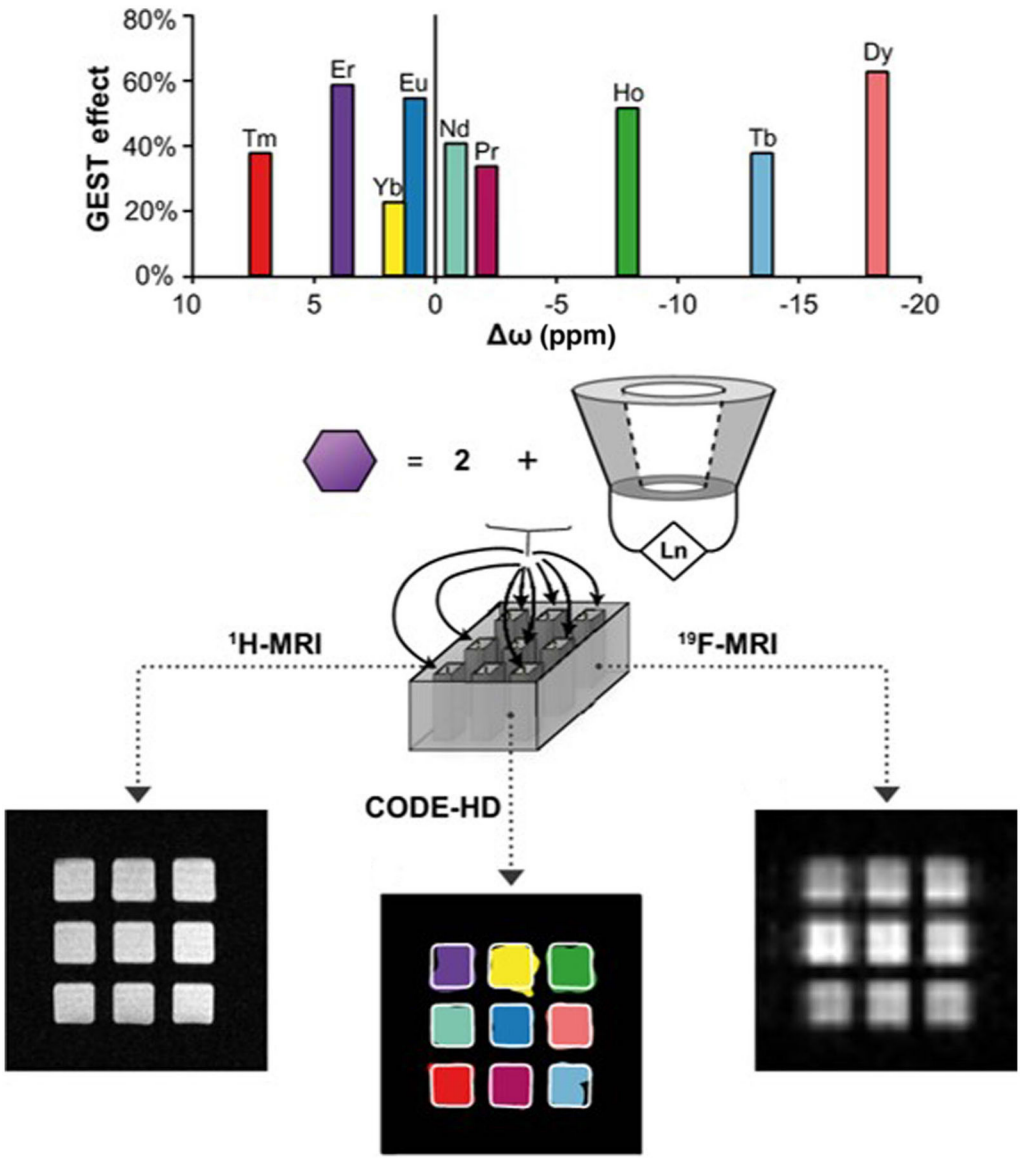

FIGURE 9.

Color display by exploiting host–guest dynamics (CODE-HD) construction and pseudocolor assignment (adapted from[45]). GEST, guest exchange saturation transfer